LEHIGH UNIVERSITY
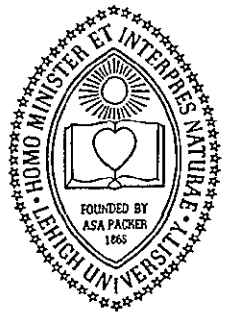
OFFICE

OF

RESEARCH

THE MONOTONIC AND CYCLIC MECHANICAL RESPONSE OF THE NI-NI$_3$NB EUTECTIC COMPOSITE

by

William R. Hoover

Department of Metallurgy and Materials Science

1970

"The Monotonic and Cyclic Mechanical Response of the

Ni-Ni3Nb Eutectic Composite"

by

William R. Hoover

A Dissertation

Presented to the Graduate Faculty

of Lehigh University

in Candidacy for the Degree of

Doctor of Philosophy

in

Metallurgy and Materials Science

Lehigh University

1970

Approved and recommended for acceptance as a dissertation
in partial fulfillment of the requirements for the degree of
Doctor of Philosophy.

May 8 1970
(date)

Professor in Charge

Accepted: _May 8, 1970_
(date)

Special Committee directing
the doctoral work of
Mr. William R. Hoover:

Chairman

ii

DEDICATION

This dissertation is dedicated to the author's wife,
Lois Elaine and his daughter, Julie Eileen, who have displayed
unremitting patience, understanding and tolerance during the
course of this research. This dissertation could not have been
possible without their help, inspiration and encouragement.

ACKNOWLEDGMENTS

TABLE OF CONTENTS

LIST OF FIGURES

ABSTRACT

The static and dynamic mechanical behavior of the Ni-Ni$_3$Nb
eutectic composite has been studied with tensile, compressive and
fatigue testing, metallography and electron fractography. In order
to more adequately understand the mechanical response of the composite,
a study of the deformation and fracture behavior of the Ni$_3$Nb phase
was also conducted.

The Ni$_3$Nb phase was found to deform primarily by twinning with
little or no slip. Under tensile loading parallel to the [100] growth
direction of the intermetallic, {112} deformation twins were formed
which subsequently served as crack nucleation sites along the {112}
twin boundaries. In addition, {011} twins developed when compression
was applied parallel to the growth direction.

Room temperature tensile testing of the Ni-Ni$_3$Nb eutectic
composite produced uniform tensile strains in excess of 11%. This
large composite ductility was attributed to extensive {112} twinning
of the Ni$_3$Nb lamellae and subsequent twin boundary cracking. When
amassed in sufficient numbers in a given cross-section, these {112}
twin boundary fissures caused composite rupture.

In an effort to more fully understand fatigue crack propagation
in composite materials, tension-tension fatigue studies of the eu-
tectic alloy were conducted. The Ni-Ni$_3$Nb composite displayed excel-
lent fatigue resistance in a notched configuration by exhibiting an

1

apparent endurance limit of about 55% of the 108 ksi smooth bar

tensile strength. Under high stress-low cycle fatigue conditions,

the fatigue resistance of the composite was controlled by the twinning

and subsequent twin boundary fracture of the Ni_3Nb reinforcing phase.

However, under low stress-high cycle fatigue conditions, Stage I crack

propagation was observed in the Ni matrix; it was, therefore, concluded

that the Ni matrix controlled the high cycle fatigue resistance of the

composite.

The fatigue behavior of the $Ni-Ni_3Nb$ eutectic composite was

compared with that of the $Al-Al_3Ni$ eutectic composite (1). The

similarity in the operative crack growth mechanisms in these two

composites suggests a trend which may apply to all composite materials.

INTRODUCTION

Space age demands for materials with increasingly superior mechanical properties will soon overcome the realistic mechanical capabilities of conventional metal alloy systems. A potential way to achieve future materials requirements involves the incorporation of high strength whiskers, fibers and blades into ductile matrices to produce composites with superior properties. To this end, an enormous amount of research has been directed toward a theoretical understanding of composite behavior and toward the ability to manufacture composite materials in an effective, economic manner. From this has come a reasonably good theoretical understanding of the static mechanical response of composites and the development of many different methods of composite fabrication.

One convenient composite manufacturing process is the unidirectional solidification of appropriate eutectic alloys (2) which can produce aligned microstructures consisting of high strength intermetallic rods or platelets imbedded in a ductile matrix. Many of these unidirectionally solidified eutectics respond mechanically as reinforced composite materials since matrix reinforcement by the high strength phase is achieved (3). Eutectic composite fabrication is accomplished by a single solidification process which is considerably easier on a laboratory scale than other composite fabrication procedures. In addition, a wide variety of composite types can be produced by simply changing eutectic alloys. It is, therefore, believed that eutectic composites provide a tractable

3

means of investigating composite behavior on a laboratory scale.

Before widespread structural usage of composite materials can be achieved, an adequate understanding of composite fatigue behavior is required. In contrast to the considerable effort devoted to composite fabrication and composite tensile behavior, only a limited number of studies have dealt with the response of fabricated composites to cyclic loading. Available data are often conflicting and confusing since a wide variety of fabricated composites, test methods and specimen geometries were used in these earlier studies (4-10). Most previous investigations have generated engineering fatigue data with little attention being given to crack growth mechanisms. Since a more thorough understanding of composite fatigue crack propagation processes is necessary before effective composite design can be achieved, more studies of fatigue fracture mechanisms are required.

The lack of extensive fatigue studies of fabricated composites is paralleled by a similar deficiency in the area of eutectic composites. Phenomenological fatigue studies conducted on the Ni-Cr (11), $Al-Al_3Ni$ (12) and $Al-CuAl_2$ (12) eutectic systems were concerned mainly with the macroscopic aspects of fatigue such as strain characteristics and cyclic lives. In another study (1), an attempt was made to understand fatigue crack propagation in an eutectic composite. This investigation showed that the $Al-Al_3Ni$ eutectic composite undergoes a fracture mechanism transition between high stress and low stress fatigue conditions. Under high stress fatigue conditions, crack propagation was controlled by the strength

4

of the Al_3Ni whiskers. However under low stress fatigue conditions,
the Al_3Ni whiskers deflected the fatigue crack and crack propagation
through the Al matrix was accomplished by a Stage I fatigue crack
propagation mechanism parallel to the reinforcing fibers. The
observation of this fracture mechanism transition has led to an
investigation of other eutectic alloys, such as the $Ni-Ni_3Nb$ eu-
tectic, to determine if such a fracture mechanism transition is
common to other eutectic composites and possibly to all composites
in general.

In earlier work, Quinn, Kraft, and Hertzberg (13) achieved
high strength levels in the unidirectionally solidified, lamellar
$Ni-Ni_3Nb$ eutectic alloy which contains 68 v/o $\alpha-Ni$ and 32 v/o
Ni_3Nb. It has been shown that both phases of this composite deform
plastically with the Ni_3Nb having been reported to slip (14) and
twin (13,15) at room temperature. The $Ni-Ni_3Nb$ eutectic composite
differs from the $Al-Al_3Ni$ composite in three basic ways: morpholo-
gy (lamellar vs. fiberous), matrix fatigue resistance and reinforc-
ing phase deformation behavior (plastically deformable Ni_3Nb vs.
elastic Al_3Ni). Since the crystallography of these two eutectics
is similar (i.e., they both possess an fcc matrix with a [110]
growth direction and a {111} interface plane with the reinforcing
phase), a realistic comparison of their fatigue crack propagation
characteristics can be made on the basis of the aforementioned
differences in morphology, matrix fatigue resistance and defor-
mation behavior of the reinforcing phases.

A detailed study of the static and dynamic behavior of the

5

Ni-Ni$_3$Nb eutectic composite will be undertaken in this investigation to provide a more complete understanding of composite fatigue crack propagation. The experimental approach will be to conduct three separate but related studies which together will produce a complete understanding of the mechanical response of the Ni-Ni$_3$Nb composite and hence, provide additional insight into composite fatigue crack growth. Initially, the deformation and fracture behavior of the Ni$_3$Nb phase will be characterized to provide an adequate understanding of the mechanical response of the constituent phases. Secondly, the monotonic characteristics of the Ni-Ni$_3$Nb composite will be established to develop knowledge of the operative monotonic fracture mechanisms. Finally, the fatigue response of the Ni-Ni$_3$Nb eutectic composite will be studied to determine the effectual fatigue crack propagation mechanisms.

THE DEFORMATION AND FRACTURE BEHAVIOR OF Ni3Nb

Introduction and Objectives

A complete understanding of the mechanical response of a composite material requires knowledge of the deformation and fracture behavior of the constituent phases. The deformation and fracture behavior of the Ni phase in the Ni-Ni3Nb composite is well understood, but the Ni3Nb phase which is expected to be the strength controlling phase of this composite is not fully characterized in terms of its mechanical behavior.

The Ni3Nb phase is an ordered orthorhombic intermetallic of type D_{2h}^{13} with lattice parameters of: $a = 5.07_9$ A, $b = 4.57_3$ A and $c = 4.23_0$ A (16). Previous investigators (14) have reported room temperature slip on two planes, one of which is the (010) plane - the other slip plane has not been identified. Quinn, et al. (13, 15) tentatively identified the formation of {112} twins in the Ni3Nb phase of the Ni-Ni3Nb eutectic when tension was applied parallel to the growth direction ([100] Ni3Nb). He also noted that cracks formed in the intermetallic near these {112} twins.

The objective of this study is to more clearly understand the deformation and fracture behavior of the Ni3Nb intermetallic phase by characterizing its twinning, slip and fracture processes.

Experimental Procedures

Specimen Preparation

Ingots of Ni3Nb with 24 a/o Nb were produced by alloying

a eutectic alloy with appropriate amounts of Nb. The composition
of 24 a/o Nb was used to simulate the room temperature composition
of the Ni_3Nb in the $Ni-Ni_3Nb$ eutectic alloy. Ingots of Ni_3Nb were
then zone refined at slow growth rates (about 5 cm/hr) to develop a
large grained structure. Subsequent X-ray orientation studies
revealed that the growth direction of the large grains produced in
this manner was [100] $\pm5°$, which is essentially coincident with the
[100] growth direction of the Ni_3Nb platelets in the $Ni-Ni_3Nb$ eu-
tectic composite (15).

Metallographic Techniques

The Ni_3Nb specimens were prepared by standard metallographic
grinding procedures with a final polish of 1 micron diamond paste.
Special care was exercised to avoid twin formation due to excessive
applied pressure during grinding ·and polishing. The specimens were
then etched in a solution of 35% HNO_3, 2% HF, and 63% H_2O. Since
no available etchant clearly delineated the pertinent grain and twin
structures under white light, most metallographic examinations were
conducted using polarized light.

Deformation Techniques

In order to examine the deformation of Ni_3Nb, closely con-
trolled deformation had to be achieved in specimens with prepolished
surfaces. Several techniques of deformation were employed for
reasons of convenience and completeness. Microhardness indentations
on prepolished surfaces were introduced to produce very severe
localized deformation. Microbend tests were conducted with the
specimen axis parallel to the [100] growth direction to produce

8

small amounts of deformation in specimens (1/8" x 1/4" x 2") with three polished surfaces. In addition, compression specimens with two prepolished surfaces parallel to the compression axis were loaded both parallel and perpendicular to the growth direction.

Trace Analysis Techniques

To facilitate subsequent trace analysis of the operative deformation mechanisms, grains in the as-grown Ni_3Nb specimens were oriented using standard Laue X-ray techniques. After straining, the deformation markings were analysed using standard one-surface and two-surface trace analysis techniques (17). Two surface trace analysis was conducted whenever possible, however, in some instances trace analysis was confined to one surface. It should be noted that due to the low symmetry of an orthorhombic lattice, one surface trace analysis in orthorhombic materials is statistically more meaningful than one surface trace analysis in cubic materials.

Results and Discussion

Examination of the deformation surface relief and the under-lying structures developed in the Ni_3Nb revealed that the operative deformation mechanisms were both unusual and complex. Efforts to develop an understanding of these mechanisms were complicated by the interaction of grown-in defects and grain boundaries with the applied stress field. To wit, a pure compressive stress state was not produced under compressive loading because regions of tensile stress were developed at appropriate defects and grain boundaries.

9

Therefore, a mixture of deformation mechanisms was always present. However, the constitution of this mixture was altered radically when the applied stress direction was changed; the determination of the stress direction required to activate the various deformation processes was thus facilitated.

Twinning

Two distinct types of twins, $\{011\}$ and $\{112\}$, were observed and analysed by trace analysis (Figure 1). The $\{011\}$ type twins were typically of a lenticular shape and were observed to be rather thick regardless of sectioning angle (Figure 2). These observations indicate that this twinning system has a relatively small twinning shear since twin offsets were always small and since the twins themselves were invariably rather wide. As many as three variants of the $\{011\}$ twin were observed in a single grain. In addition, it was found that the $\{011\}$ twins formed when a compressive stress was applied parallel to the $[100]$ growth direction.

In contrast to the $\{011\}$ twins, the $\{112\}$ twins were observed to form along any of four variants when tensile stresses were developed parallel to the growth direction. These $\{112\}$ twins always appeared as very narrow, straightsided twins (Figure 3) and as such were easily distinguishable from the $\{011\}$ twins. The very small twin widths, large twinning offsets and the tendency for crack initiation along twin boundaries indicate that the twinning shear in the $\{112\}$ twins is very high.

Due to the small twin widths, trace analysis of the $\{112\}$ twins was limited to one surface. These data are believed suf-

10

ficient since Quinn (15) tentatively identified this twinning

system previously and since orthorhombic one surface trace analyses

are statistically superior to cubic one surface trace analyses.

Since the differences between the $\{011\}$ twins and the $\{112\}$

twins play an important role in the deformation of the Ni_3Nb phase

(both in the $Ni-Ni_3Nb$ eutectic and by itself), the following table

is useful as a means of providing a direct comparison and a summary

of their characteristics.

	$\{011\}$ Twins	$\{112\}$ Twins
Stress Requirement	Compression parallel to growth direction	Tension parallel to growth direction
Shape	lenticular	straight-sided
Size	thick	thin
Offset Size	small	large
No. variants observed	3	4
Inferred twinning shear magnitude	low	high

Slip

Although slip has been reported previously for the Ni_3Nb

phase (14,15) no slip could be observed optically during this study

under any loading condition. The regions which appeared to have

slipped when observed at low magnifications (as in Figure 4) are

seen to be rows of extremely fine twins when examined using high

magnifications and polarized light as shown in Figure 5. The

conclusion that these are twins is based on the observations that

11

they possess a finite width, do not polish off, and are a different color than the surrounding matrix, indicating a different crystallographic orientation. It would be easy to mistake these twins as slip traces unless careful high magnification examination was conducted. The reported observations of slip may either be due to incorrect identification or possible compositional variations in the Ni_3Nb phase which could activate different deformation mechanisms. In addition, it is possible that homogeneous slip occurs in this alloy on such a fine scale that it can not be observed optically.

Slip may not be expected in Ni_3Nb even though twinning is observed. It is known that an ordered alloy will have less tendency to slip and twin than a disordered alloy since such deformation processes may disrupt the crystallographic order. Examination of the Ni_3Nb crystal structure reveals that no obvious planes exist where passage of a perfect dislocation could occur without bringing two Nb atoms into adjacent positions. Slip may therefore be unlikely since it would require Nb atoms to become first nearest neighbors. However, it is possible that twinning can occur without bringing Nb atoms into adjacent positions. Twinning will most likely change only the second nearest neighbor relationships and, therefore, could be more energetically favorable than slip.

Fracture

Examination of fractured Ni_3Nb bend specimens revealed that fracture is initiated at and propagates along {112} twin boundaries.

12

Cracks around hardness indentations and fissures in compression specimens also indicate that the {112} twin boundaries provide easy locii for crack initiation and propagation. Under compressive loading, final fracture of the Ni₃Nb is preceded not only by incipient cracks along {112} twin boundaries but by grain boundary cracking as well (Figure 4).

In contrast to the {112} twins which play a vital role in Ni₃Nb fracture, the {011} twins were observed to be inactive in the fracture process. Cracking and subsequent fracture along {011} twin boundaries were never observed. This behavior is consistent with the small twinning shear associated with {011} twinning.

Summary of Ni₃Nb Behavior

It has been shown that the primary deformation mechanism in Ni₃Nb is twinning along {112} planes when tension is applied parallel to the [100] growth direction and along {011} planes when compression is applied parallel to the growth direction. The {112} twin boundaries provide the primary location for crack initiation and propagation. Grain boundary cracking is observed occasionally especially under compressive loading. No optical evidence of slip could be developed in contrast to previously reported findings (14,15).

13

THE MECHANICAL RESPONSE OF THE Ni-Ni$_3$Nb EUTECTIC COMPOSITE

Introduction and Objectives

Since an understanding of the Ni$_3$Nb deformation and fracture behavior has been developed, a detailed study of the mechanical response of the Ni-Ni$_3$Nb eutectic composite is now feasible. The objective of this research effort is to determine the monotonic and cyclic behavior of the Ni-Ni$_3$Nb eutectic composite and to relate this behavior to the properties of the constituent phases. Particular emphasis will be placed on crack growth mechanisms during both static and dynamic loading conditions.

Experimental Procedures

Specimen Preparation

Master heats of Ni-23.3 w/o Nb using high purity materials (99.97% Ni and 99.7% Nb) were induction melted under an argon atmosphere and cast into steel chill molds. (For a detailed description of the melting practice, see Appendix I.) The cast ingots, contained in Al$_2$O$_3$ crucibles and covered with a dynamic argon atmosphere, were then unidirectionally solidified vertically using induction heating. Although most specimens were grown at 4.7 cm/hr, specimens for growth rate studies were grown at 2.75 cm/hr, 4.7 cm/hr, 8.3 cm/hr and 13.3 cm/hr.

Testing Procedures and Equipment

Tensile testing of standard 1/4 inch diameter tensile

specimens was conducted with a strain gauge extensometer measuring the strain over the one inch gauge length. In addition, notched tensile tests were performed on standard 1/4 inch diameter tensile samples with a 60° notch in the center of the gauge section which reduced the cross-sectional area by 45%. (The measured notch root radius was less than 0.003 inches.) Compression tests were also conducted with 0.200 inch diameter by 0.500 inch high cylinders of the eutectic. All testing was conducted parallel to the growth direction on an Instron testing machine with a cross-head rate of 0.02 inches/minute. A summary of the results of this static testing program is given in Table I.

To insure consistency in crack nucleation and thereby give a strong measure of the material's crack propagation characteristics, the previously described notched tensile specimens were also used in the tension-tension fatigue studies. The fatigue tests were performed on an MTS Testing System with a frequency range of 3-40 cps and a minimum net section stress of 2,000 psi.

Metallographic and Fractographic Techniques

After testing, appropriate specimens were nickel plated and sectioned longitudinally for metallographic examination of the fracture profile. Two different metallographic preparation techniques were used to produce the desired results. Technique A was used for all fracture profile studies. With this technique, Ni_3Nb twinning was observable only under polarized light while Technique B produced microstructures which clearly showed the Ni_3Nb twins

15

under white light. Technique A was used almost exclusively in this study because it produced a metallographic polish free of excessive surface relief and edge rounding. All micrographs included in this work are of specimens prepared by Technique A unless otherwise noted. (See Appendix II for a detailed description of the metallographic preparation techniques.)

Fractographic examination of the fracture surfaces was conducted when appropriate. A standard two-stage carbon replica technique was employed using a Pt-C shadowing material. The replicas were examined on an RCA EMU 3G electron microscope operated at an accelerating potential of 50 kv.

Results and Discussion

Structure

The initial unidirectional solidification of the $Ni-Ni_3Nb$ eutectic was conducted over a range of growth rates (2.75, 4.7, 8.3, and 13.3 cm/hr) to find the optimum growth rate for subsequent detailed mechanical behavior studies. As expected, the lamellar size and eutectic grain size decreased with increasing growth rate. However, microstructural alignment and Ni_3Nb platelet uniformity were best at the growth rate of 4.7 cm/hr.

Since the growth rate to be selected for further study should be based on mechanical properties as well as microstructure, tensile tests were conducted on specimens grown at various growth rates. The data (Figure 6) show a lack of a strength dependency on growth rate which is unusual for eutectic composites. (A discussion of

16

this unusual behavior will be deferred until later.) Therefore, a growth rate of 4.7 cm/hr was selected for detailed mechanical property studies since it represented the best combination of eutectic grain size, lamellar width, platelet uniformity and microstructural alignment. The transverse microstructure obtained at this growth rate is shown in Figure 7.

Monotonic Behavior

Monotonic Properties

Tensile tests of the $Ni-Ni_3Nb$ composite illustrate the unusual properties of this material. A typical tensile stress-strain curve given in Figure 8 reveals the composite yielding behavior* and the large elongation under constant stress which characterizes the tensile behavior of this composite. The large tensile ductility ($>$11%) demonstrated by the $Ni-Ni_3Nb$ composite (Table I) far exceeds the ductility of only a few percent normally observed for metal matrix composites. These results are particularly interesting since Quinn (15) previously observed almost negligible ductility for this eutectic composite.

The extensive tensile ductility displayed by the $Ni-Ni_3Nb$ composite suggests that notch strengthening may occur. Indeed, the notched tensile strengths (Table I) exceed the smooth bar strengths by more than 25%. This demonstrated notch strengthening is much

---

*In this dissertation, the term composite yielding will refer to the plastic-plastic yielding of both phases of the composite as distinguished from elastic-plastic or only matrix yielding.

larger than has ever been achieved in a metal matrix composite at room temperature: most composites are considered "tough" if the room temperature notched strength ratio approaches 1.0.

In spite of its apparent ductility, the Ni-Ni$_3$Nb composite does not neck prior to tensile fracture. To wit, the observed reduction in area is uniform over the entire gauge section and is approximately equal to the total uniaxial strain (Table I).

The compressive properties of Ni-Ni$_3$Nb (Table I) indicate that the ultimate compressive strength is more than twice the ultimate tensile strength. An explanation for this strength differential can be obtained from a study of the operative deformation mechanisms in the Ni$_3$Nb phase as will be discussed subsequently.

Tensile Deformation Characteristics

Metallographic examination of smooth bar tensile fractures revealed extensive twinning and cracking of the Ni$_3$Nb phase throughout the entire gauge length (Figure 9). Using trace analysis techniques, the Ni$_3$Nb twins were identified as multiple variants of the {112} twin. Careful metallographic studies also showed that the observed cracks were actually Ni$_3$Nb twin boundary fissures. Both the {112} twinning and the subsequent twin boundary cracking are consistent with the previous deformation studies conducted on the Ni$_3$Nb phase.

To more precisely understand the roles of twinning and twin boundary cracking in the deformation of this composite and to determine the extent to which each occurs, a series of tensile specimens

were elongated to different amounts of tensile strain. After
straining, each specimen was sectioned longitudinally and the
entire gauge section examined metallographically. To obtain the
average volume percent of the Ni_3Nb twinned, a point counting tech-
nique was employed throughout the entire gauge section. Lineal
analysis was also conducted over the gauge length to determine the
average number of cracks per unit length per Ni_3Nb lamellae.

The results of the quantitative metallography (Figure 10)
indicate that initial composite yielding behavior is due to the
onset of Ni_3Nb twinning. Before yielding (which occurs at approxi-
mately 0.4% strain), no twinning of the Ni_3Nb is observed. How-
ever, after yielding a significant amount of {112} twinning is
present in the Ni_3Nb. (The composite yielding behavior is believed
to be controlled by the Ni_3Nb phase since the Ni matrix is expected
to yield at a stress below the composite yield stress.) {112}
twinning accounts for all the elongation up to about 4% strain.
Strains in excess of 4% are produced by Ni3Nb twin boundary crack-
ing as well as {112} twinning.

Although twin boundary cracking contributes to the strain
achieved in the composite, extensive {112} twinning throughout the
gauge section must be considered of major importance. Without the
ability to twin throughout the gauge section at a relatively
constant stress level, deformation damage would be localized and
premature composite fracture would occur.

The capability of the Ni3Nb phase to twin throughout the gauge
section is intimately related to the crystallography of the {112}

19

twinning process. Due to the symmetry of the {112} planes about

the [100] growth direction, all {112} planes in every Ni$_3$Nb

lamellae experience an equal shear stress at any given load level.

Therefore, multiple twinning can occur when the applied load pro-

duces the critical shear stress for {112} twinning. To wit, when

{112} twin formation begins, it can occur at the same stress level

in all eutectic grains and on all {112} twin variants (if the

twinning senses are correct) with equal ease. Thus {112} twin

formation can occur throughout the entire gauge section at a

constant stress level. It is this extensive twin formation and the

subsequent twin boundary cracking which account for the large e-

longations at essentially constant stress which follow the Ni-Ni$_3$Nb

composite yielding.

Tensile Fracture Behavior

Although the Ni-Ni$_3$Nb composite displays considerable ductili-

ty, tensile fracture surfaces are macroscopically flat (normal to

the loading axis) with a total absence of shear lips. As expected,

the deformation mechanism of {112} twinning and twin boundary

cracking plays a key role in the tensile fracture behavior of this

composite material. Examination of metallographic fracture profiles

(Figure 11) indicates that final composite rupture is achieved by

Ni$_3$Nb failure along twin boundaries and subsequent necking of the

intervening Ni lamellae. Figure 11 illustrates that all the Ni$_3$Nb

lamellae break parallel to incipient secondary cracks which are

known to be twin boundary fissures. The Ni matrix is character-

istically necked between the Ni$_3$Nb lamellae although shear failure

of the Ni matrix is occasionally observed in a fashion similar to that noted by Hertzberg, Lemkey and Ford (18) in the Al-CuAl$_2$ eutectic composite.

It is apparent that tensile fracture of the Ni-Ni$_3$Nb eutectic composite is affected by a sequence of events. After the initial stages of elastic deformation and matrix yielding, the Ni$_3$Nb phase begins to twin along $\{112\}$ planes which gives rise to the composite yielding behavior. Upon further deformation, Ni$_3$Nb twinning and the ensuing twin boundary cracking spread throughout the gauge section. When a sufficient number of twin boundary fissures are amassed in a given cross-section, the increased local stress level leads to final composite fracture by rupture of all Ni$_3$Nb platelets and the subsequent necking of the Ni matrix.

This proposed tensile fracture mechanism has been confirmed by fractographic studies. The tensile fracture surfaces were found to consist of Ni$_3$Nb platelets which had ruptured in a flat, brittle manner with the Ni matrix necked in between. Figure 12 is a typical fractograph of a tensile fracture showing the necked Ni matrix flanked on either side by broken Ni$_3$Nb platelets.

Tensile fractographic studies also revealed the frequent presence of tongues and steps on the fracture surfaces of the Ni$_3$Nb platelets (Figure 13). These features were observed to lie at angles of approximately 0°, 40° and 90° to the Ni-Ni$_3$Nb interface. The formation of these tongues and steps is believed related to the possible presence of four variants of the $\{112\}$ twin in a Ni$_3$Nb lamellae (Figure 14). If fracture occurs along one twin variant,

21

the other three variants, when present, will intersect the fracture surface. The three possible twin instersections with the {112} fracture surface occur at angles of·0°, 43° and 90° to the Ni-Ni₃Nb interface as depicted in Figure 15. The observed steps and tongues are, therefore, believed to be the manifestations of the inter-section of secondary {112} twins with the fracture surface. The tongues are formed by cracks along the secondary twins while the steps reflect the orientation change in the fractured twin boundary caused by an intersecting secondary twin.

Summary of Tensile Behavior

Having examined the tensile deformation and fracture character-istics of the Ni-Ni₃Nb composite, it is clear that the unusually large composite ductility and the distinctive composite yielding be-havior is a direct reflection of the {112} deformation twinning of the Ni₃Nb phase and subsequent twin boundary cracking. These twin boundary fissures initiate final composite rupture when a sufficient number are amassed in a given cross-section.

The tensile fracture of the Ni-Ni₃Nb eutectic composite is believed to be controlled by a deformation process (i.e. the tensile fracture process is initiated by {112} deformation twinning of 'the Ni₃Nb). Deformation controlled fracture is basically different from the fracture mechanisms observed in composites with elastic reinforcing phases. In these whisker-like composites, the strength of the reinforcing phase controls the fracture process. The rami-fications of this subtle difference in fracture mechanism will be discussed in the ensuing section.

22

Growth Rate Effects on Tensile Behavior

As has been discussed previously, the usual increase in strength with increasing growth rate was not observed for the Ni-Ni$_3$Nb eutectic composite. Within experimental error, the tensile strength was found to remain constant over a range of growth rates from 2.7 cm/hr to 13.3 cm/hr (Figure 6). The explanation for this behavior is believed based on the fact that Ni-Ni$_3$Nb composite failure is deformation controlled.

In composites with whisker-like reinforcing phases, a significant increase in tensile strength is usually observed as the size of the reinforcing phase is decreased (volume fraction held constant). This effect is believed to be due largely to an increase in the statistical probability that the reinforcing whiskers will be more perfect when present in smaller diameters. When composite fracture is deformation controlled, the strength of the reinforcing phase should not be a function of size. However, refinement of the composite microstructure may cause strength increases due to effects such as additional mechanical constraint and increased dispersion hardening of the matrix by the reinforcing phase. Since the Ni-Ni$_3$Nb composite shows no significant increase in strength over the size range studied, it is apparent that microstructural refinement does not affect the basic fracture mechanism of {112} twinning and subsequent twin boundary cracking. The lack of a strength dependency on growth rate in the Ni-Ni Nb composite is believed to be a consequence of the deformation controlled fracture process which operates in this material.

23

Compressive Behavior

The Ni-Ni$_3$Nb eutectic composite has been observed to be much stronger in compression than in tension. To understand this behavior, compression specimens were macroscopically and metallographically examined after deformation. Metallographic examination of the specimens which had failed by macroscopic barreling and/or kinking, revealed that the Ni$_3$Nb lamellae deformed by {011} twinning. (No evidence of {112} twinning was found.) However, in contrast to the {112} twin boundary cracking observed under tensile loading, no {011} twin boundary cracking was observed. The presence of {011} twins which did not nucleate twin boundary cracks is consistent with the previous Ni$_3$Nb deformation studies.

Under tensile loading conditions, composite failure was precipitated by cracks which nucleated at the {112} twin boundaries. However, the {011} twins formed in compression showed no tendency for crack initiation at the twin boundaries. Therefore, the superior compressive strengths can be accounted for by the absence of a compressive deformation mechanism which creates preferred sites for crack nucleation.

Summary of Monotonic Behavior

This detailed study of the monotonic deformation and fracture of the Ni-Ni$_3$Nb eutectic composite has shown that all of the observed static properties depend on the {112} deformation twinning of the Ni$_3$Nb phase and subsequent twin boundary fracture. As such, the tensile fracture of the material is considered to be deformation controlled. The observed deformation and fracture processes explain

24

and account for the large tensile ductility, the notch strengthening, the shape of the tensile stress-strain curve, and the compressive strengths which far exceed the tensile strengths.

Fatigue Behavior

Fatigue Results

The S-N curve (Figure 16) developed during the fatigue study illustrates several unusual characteristics of the Ni-Ni$_3$Nb eutectic composite. The composite displays significant cyclic lives at stress levels above the smooth bar tensile strength. Although this high stress fatigue resistance would be unexpected for a typical "brittle" composite, it is understandable in view of the notch strengthening displayed by this composite. In addition to good high stress fatigue properties, the Ni-Ni$_3$Nb composite has an apparent endurance limit for a notched configuration at a net section stress level of about 60 ksi. Since a smooth bar endurance limit of 55% of the smooth bar tensile strength is quite good for nickel based alloys, the observed notched endurance limit of 55% of the tensile strength must be considered outstanding.

Metallographic Observations

Metallographic examination of fatigue specimens tested at various levels of alternating stress revealed several systematic changes in the fracture profile appearance. As the level of alternating stress was decreased, the extent of {112} twinning in the Ni$_3$Nb became more limited to the vicinity of the fracture surface. This localization of the Ni$_3$Nb twinning was also accompanied by an

25

anticipated decrease in the number of secondary twin boundary cracks. The less severe crack tip stress environment at the lower alternating stress levels restricted the deformation damage to the region immediately adjacent to the fracture surface. This concentration of deformation damage continued until at a stress level of 65 ksi (562,800 cycles to failure) virtually no {112} twins and twin boundary fissures were observed away from the fracture surface itself. Figure 17 represents a typical area in the fracture profile of a specimen tested at the 65 ksi level. Note the absence of any twin boundary cracks and the lack of any evidence of {112} twinning away from the fracture surface. (Examination under polarized light reveals no twins except at the fracture surface.) In addition, Figure 17 reveals that the Ni matrix does not exhibit a neck profile. Instead of necking as observed under high stress conditions, the Ni matrix appears to fracture along straight facets which are not clearly resolvable using light microscopy.

Fractographic Observations

Under high stress-low cycle fatigue conditions (cyclic lives of less than 2,000 cycles), fractographic analysis indicated that the Ni$_3$Nb lamellae fracture in advance of the crack front. The voids created by these fractured Ni$_3$Nb lamellae grow sequentially under the influence of the cyclic stress until impinging on adjacent voids. This crack growth by cyclically induced void growth and coalescence is characterized by the presence of fatigue striations on the intervening necked Ni matrix which always lie parallel to the Ni-Ni$_3$Nb interface as shown in Figure 18. This high stress

26

fatigue fracture mechanism is controlled by the Ni$_3$Nb twinning and subsequent twin boundary cracking process which was observed under tensile conditions. Fracture occurs in the same basic manner as does tensile fracture except the necking of the intervening Ni lamellae is observed to occur sequentially by striation formation under the applied cyclic stress.

The fatigue fracture mechanism under intermediate stress conditions (cyclic lives of 2,000 to 20,000 cycles) is observed to be somewhat different. Under the influence of an intermediate alternating stress, the Ni$_3$Nb lamellae do not rupture in advance of the crack tip. Rather, the fractured Ni$_3$Nb platelets lead the crack front under this condition as fingers of fractured material protruding into the unfractured Ni matrix. The Ni lamellae fail in fatigue under the influence of cracks on three sides--the two adjacent Ni$_3$Nb lamellae and the macroscopic crack front. This process produces striations on the Ni necks which approach the Ni-Ni$_3$Nb interface in an asymptotic fashion as seen in Figure 19.

A radical change in the fracture surface appearance is noted on low stress-high cycles fatigue fracture surfaces (greater than 20,000 cycles to failure). The Ni matrix fails in a faceted manner (Figure 20) rather than by necking as observed previously. In addition to the faceted Ni fracture surface which contained no evidence of fatigue striations, a decrease was observed in the number of steps and tongues on the Ni$_3$Nb fracture surfaces. Both the observed faceted Ni fracture surfaces and the decrease in

27

tongues and steps are consistent with the metallographic obser-
vations of an absence of Ni neck profiles and a lack of secondary
twins in the Ni_3Nb adjacent to the fracture surface.

Although the faceted appearance of the Ni matrix was not
anticipated, similar faceted fracture surfaces were observed by
Gell and Leverant (19,20) in the Ni-based superalloy MAR-M200.
Gell and Leverant were able to identify the operating fracture
mechanism as Stage I fatigue crack propagation along active slip
planes. Hence, the facets observed by Gell and Leverant were 111
planes.

There are several reasons for the belief that Stage I crack
propagation is a plausible explanation of the faceted Ni fracture
surfaces observed in this composite under high cycle fatigue
conditions. First, one set of the facets are observed to lie
parallel to the Ni-Ni_3Nb interface which is known to be a $\{111\}$
plane in the Ni (15). In addition, the other facets lie approxi-
mately 70.5° and 109.5° from the interface and are, therefore,
believed to be $\{111\}$ planes also. However, since electron fracto-
graphs are projections which are not necessarily angularly accurate,
this is circumstantial evidence.

In an effort to conclusively prove that the facets on the Ni
fracture surfaces under low stress fatigue conditions are due to a
Stage I crack growth mechanism, etch pit studies on the fracture
surface were conducted. Exploratory work with metallographic speci-
mens of Ni revealed that etching in a boiling solution of 1 1/2
parts H_2SO_4, 2 1/4 parts HNO_3, 1 part H_2O and NaCl produces etch

28

pits in the Ni. Examination of these etch pits using both anneal-
ing twins and slip traces indicated that the facets developed in
the etch pits were {111} planes. This exploratory work also indi-
cated that etch pitting did not occur unless the etched surface was
very close to a {111} plane. To wit, etch pits were always observed
to be nearly perfect equilateral triangles.

Difficulty was encountered in attempts to etch pit the high
cycle fracture surfaces. The dislocation density in the Ni phase
was very high. Consequently, the etch pits which formed on the
fracture surface were so close together that the underlying fracture
surface identity was almost entirely obliterated. In addition, well
defined etch pit facets were rarely observed due to the close prox-
imity of neighboring etch pits. Although it was not possible to
show that the facets on the fracture surface lie parallel to the
{111} etch pit facets, the presence of etch pits in such large
numbers indicates that the facets of the Ni fracture surface are
either {111} planes or very nearly {111} planes.

The combination of the aforementioned evidence (Gell and
Leverant observations, facet orientations and the etch pit studies)
suggests that crack growth through the Ni matrix under low stress
fatigue conditions occurs by a Stage I crack propagation mechanism.

The metallographic and fractographic observations suggest that
Stage I crack propagation through the Ni matrix controls the low
stress-high cycle fatigue resistance of this alloy. It is believed
that as the fatigue crack approaches the Ni-Ni$_3$Nb interface by
Stage I crack propagation through a Ni lamellae, the crack tip stress

29

field induces the formation of a {112} twin in the adjacent Ni_3Nb

platelet. This twin subsequently fractures along the twin boundary

enabling fatigue crack growth to continue across the next Ni

lamellae. Thus, the rate of low stress fatigue crack propagation

through the composite is controlled by the rate of Stage I fatigue

crack propagation through the Ni matrix. It is, therefore, con-

cluded that the low stress-high cycle fatigue resistance of the

$Ni-Ni_3Nb$ eutectic composite is controlled by the Ni matrix.

Summary of Fatigue Behavior

This study of the fatigue behavior of the $Ni-Ni_3Nb$ eutectic

composite has clearly shown that a fatigue fracture mechanism

transition occurs between high stress and low stress fatigue

conditions. Under high stress-low cycle fatigue conditions, crack

growth is accomplished by sequential void growth by striation

formation leading to their eventual coalescence. Hence, the high

stress fatigue resistance is controlled by fracture of the Ni_3Nb

phase. However, under low stress-high cycle fatigue conditions,

fatigue crack growth through the Ni matrix is believed to occur by

a Stage I crack propagation mechanism. It is, therefore, considered

that the low stress fatigue resistance of the $Ni-Ni_3Nb$ eutectic

composite is controlled by the resistance of the Ni matrix to Stage

I crack propagation along active slip planes.

Comparison of Results with Quinn's Results

In previous work on the $Ni-Ni_3Nb$ eutectic composite (13,15)

Quinn surveyed the room temperature tensile behavior and tentatively

identified the {112} twinning which occurs under tensile loading

30

conditions. Although Quinn apparently observed the same fracture mechanism, his specimens of the Ni-Ni$_3$Nb eutectic composite displayed slightly higher strengths (110-130 ksi) and very limited ductility. Why did Quinn's specimens, which failed by the same basic mechanism, display such different mechanical properties? Due to equipment limitations, Quinn was forced to use horizontal unidirectional solidification. Consequently, his specimens possessed a degree of microstructural misalignment which he estimates to be $\pm 10°$ (max.). The explanation for the observed discrepancies in mechanical behavior lies in the misalignment present in Quinn's samples.

In Quinn's horizontally grown ingots, the applied stress required to initiate twinning varied from eutectic grain to eutectic grain because of the misalignment. In grains even slightly misaligned (tensile axis not parallel to [100]), all the {112} twin variants were not equally favored due to nonsymmetrical loading. This misalignment in the horizontally grown specimens caused Ni$_3$Nb twinning to occur over a range of applied stress levels which most likely led to the slight increase in strength over the vertically grown specimens.

The misalignment in the horizontally grown samples could have limited the observed ductility in two ways. First, not all twin variants were equally active in each Ni$_3$Nb lamellae, therefore, there was less capability to deform. Secondly, misalignment may have caused specific eutectic grains to experience severe deformation damage (Ni$_3$Nb twinning and twin boundary cracking) before

31

the surrounding grains twinned extensively. These pockets of very

severe damage could have caused premature composite failure.

The different behaviors displayed by the vertically and hori-

zontally grown specimens of the Ni-Ni$_3$Nb eutectic serves as an

example of the influence of microstructural alignment on composite

mechanical behavior. By achieving slightly better alignment, a

brittle, high strength composite was transformed into a very ductile

(tough) composite of only slightly lower strength level.

Comparison with the Al-Al$_3$Ni Eutectic Composite

Although both the Al-Al$_3$Ni and Ni-Ni$_3$Nb eutectic composites

have fcc matrices which grow in a [110] direction, these two eu-

tectic composites are quite different in terms of their morphology,

their matrix fatigue resistance and their reinforcing phase defor-

mation behavior. In spite of the above differences, a comparison

of the fatigue behaviors of these two composites, reveals a sur-

prising similarity. Under high stress fatigue conditions, fatigue

crack growth was controlled by the reinforcing phase in both the

Al-Al$_3$Ni and the Ni-Ni$_3$Nb eutectic composites. When subjected to

low stress fatigue, crack growth through the matrix in both eutectic

systems was observed to occur by Stage I fatigue crack propagation.

It is, therefore, believed that the matrix controls the high cycle

fatigue resistance in both the Al-Al$_3$Ni eutectic composite and the

Ni-Ni$_3$Nb eutectic composite even though the Al$_3$Ni fibers deflected

the fatigue crack and the Ni$_3$Nb platelets did not. The trend de-

veloped in these two eutectics is that crack growth changes from a

reinforcing phase controlled mechanism to a matrix controlled mecha-

32

nism as the level of alternating stress is decreased.

CONCLUSIONS

1. Deformation of the Ni_3Nb phase is accomplished primarily by deformation twinning. {112} twinning is observed when a tensile stress is applied parallel to the [100] growth direction and {011} twins are formed when compression is applied parallel to the growth direction.

2. Tensile fracture of the Ni_3Nb phase initiates at and propagates along {112} twin boundaries. Grain boundary fracture is occasionally observed especially under compressive loading.

3. The unique ductility of the $Ni-Ni_3Nb$ eutectic composite is due to the {112} deformation twinning of the Ni_3Nb lamellae and subsequent twin boundary cracking.

4. The tensile fracture of the $Ni-Ni_3Nb$ eutectic composite is controlled by a deformation process: {112} twinning of the Ni_3Nb phase.

5. The high stress-low cycle fatigue resistance of the $Ni-Ni_3Nb$ eutectic composite is controlled by fracture of the Ni_3Nb phase.

6. Low stress-high cycle fatigue crack growth occurs in the Ni matrix by a Stage I crack propagation mechanism. Consequently, the low stress fatigue life of the $Ni-Ni_3Nb$ eutectic composite is considered to be controlled by the Ni matrix.

33

7. When compared with the Al-Al3Ni eutectic composite, the
   Ni-Ni3Nb composite displays a similar fatigue behavior
   even though the two composites are quite different.
   The high stress fatigue lives of both eutectic composites
   -is controlled by the strength of the reinforcing phase
   and the low stress crack propagation in the matrix occurs
   by Stage I fatigue crack propagation.

Appendix I - Melting Procedures

Master heats of the Ni-Ni$_3$Nb eutectic were produced in 1800 gram quantities using an Al$_2$O$_3$ crucible under a dynamic argon atmosphere. Induction heating was conducted in such a manner as to achieve melting in approximately 20 minutes. The melt was held for 10 minutes to allow homogenization and then cast into a steel chill mold. The steel mold was designed in a split-mold fashion to allow production of eight 1/2 inch diameter by 8 inches long ingots. To prevent seizing, the steel mold was coated with a MgO slurry prior to each casting.

Although the most recently reported eutectic composition for the Ni-Ni3Nb system is 23.3 w/o Nb (13), initial melts charged to this composition were ·found to be rich in Ni$_3$Nb. This discrepancy was due to either an error in the reported eutectic composition or the vaporization of nickel. Although the vapor pressure of nickel in the temperature range of interest is relatively low, the exo-thermic reaction caused when Nb is dissolved in the molten Ni raises the local bath temperatures causing hot spots of significantly higher temperatures. To overcome this problem and to insure con-sistency from heat to heat, all the Nb in the form of one inch squares of 0.010 inch thick sheet was placed at the bottom of the crucible underneath 1 1/2 inch square pieces of 1/2 inch thick Ni slabs. This charging technique allowed for uniform melting pro-cedures (power input and melting time) and consistent nickel losses during melting.

To determine the charging composition required to achieve the metallographically determined eutectic composition, a series of various charging compositions were used. It was found that a charging composition of 22.3 w/o Nb (1 w/o Ni rich) produced both as-cast and controlled microstructures which were typically eutectic in nature.

Appendix II - Metallographic Techniques

As discussed under Experimental Procedures, two different preparation techniques were used to prepare specimens of Ni-Ni$_3$Nb for microstructural examination.

Technique A

In this preparation technique, the specimens were wet ground through 600 grit; rough polished with one micron diamond paste and fine polished with Linde B (Al$_2$O$_3$). The specimens were then immersion etched for about eight seconds in a modified Marbles Reagent (20g, CuSO$_4$; 100ml, HCl (conc.); 100ml H$_2$O; and 200ml, ethyl alcohol).

Specimens prepared by this technique had good edge retention and minimal surface relief and were, therefore, used for high magnification studies of fracture surface profiles. However, the twins in the Ni$_3$Nb phase which were of paramount interest were observable only under polarized light. Thus, this technique was unsatisfactory for photographically recording the Ni$_3$Nb twins due to the very low contrast developed under polarized light. It was with this problem in mind that the development of Technique B was undertaken.

Technique B

In this technique, specimens were prepared in an analogous fashion to Technique A except the final polishing was conducted using MgO in a Syntron vibratory polisher for one hour. Upon etching in the aforementioned modified Marble's Reagent, the Ni$_3$Nb

twins were readily observable under white light and hence easily photographed. The difficulty with Technique B is that the excessive final polishing developed too much surface relief and edge rounding for high magnification examinations. Therefore, Technique B was limited to relatively low magnification examinations of the twinned structures. (Technique B was used in Figure 9 and Technique A was used for the remainder of the micrographs in this dissertation.)

TABLE I

Monotonic Properties of the Ni-Ni$_3$Nb Composite

PROPERTIES	AVERAGE RESULTS	RANGE OF RESULTS	NO. OF TESTS
ULTIMATE TENSILE STRENGTH, ksi	108.7	104.7 - 115.0	9
STRAIN AT TENSILE FRACTURE, %	12.4	11.25 - 15	4
REDUCTION IN AREA, %	13.4	11.7 - 16.8	3
NOTCHED TENSILE STRENGTH, ksi	139.8	138.0 - 143.4	3
ULTIMATE COMPRESSIVE STRENGTH, ksi	234.7	222.3 - 254.1	7
COMPRESSIVE STRAIN AT ULTIMATE, %	6.03	4.96 - 6.89	7

REFERENCES

1. W. R. Hoover and R. W. Hertzberg, "The Fatigue Characteristics of Unidirectionally Solidified Al-Al$_3$Ni Eutectic Alloy," Trans. ASM, v. 61, (1968), p. 769.

2. R. W. Kraft and D. L. Albright, "Microstructure of Unidirectionally Solidified Al-CuAl$_2$ Eutectic," Trans. AIME, v. 221, (1961), p. 95.

3. R. W. Hertzberg, "Potential of Unidirectionally Solidified Eutectic Alloys as Reinforced Composites," Fiber Composite Materials, ASM, Metals Park, Ohio, (1965), p. 77.

4. A. A. Baker, "The Fatigue of Fibre-Reinforced Aluminum," J. of Mat'ls Sci., v. 3, (1968), p. 412.

5. A. W. H. Morris and E. A. Steigerwald, "An Investigation of the Fatigue Behavior of Tungsten-Reinforced and Steel-Reinforced Silver Composites," Trans. AIME, v. 239, (1967), p. 730.

6. P. J. E. Forsyth, R. W. George and D. A. Ryder, "Some Preliminary Tests on Al Alloy Sheets Reinforced with Strong Wires," Applied Mat'ls. Res., v. 3, (1964), p. 223.

7. R. K. Ham and T. A. Place, "The Failure of Cu-W Fibre Composites in Repeated Tension," J. Mech. Phys. Solids, v. 14, (1966), p. 271.

8. A. A. Baker, J. E. Mason and D. Cratchly, "High Strain Fatigue Studies of a Composite Material," J. of Mat'ls. Sci., v. 1, (1966), p. 229.

9. A. A. Baker, "The Effect of Fiber Diameter and Discontinuous Fibers on the Fatigue of a Fibre-Reinforced Metal," Applied Mat'ls Res., v. 5, (1966), p. 210.

10. R. C. Donat, "Fatigue Tests on a Boron-Epoxy Laminate," J. of Composite Mat'ls., v. 4, (1970), p. 124.

11. K. Sadananda and J. C. DiPrimio, "High Strain Fatigue of an Eutectic Ni-Cr Unidirectionally Solidified Alloy with Lamellar Structure," paper presented at the 1969 Spring Meeting of The Metallurgical Society of the AIME.

12. M. J. Salkind, F. D. George, F. D. Lemkey and B. J. Bayles, "An Investigation of the Creep, Fatigue, and Transverse Properties of Al$_3$Ni Whisker and CuAl$_2$ Platelet Reinforced Aluminum," United Aircraft Research Laboratories, Final Report, Contract Now 65-0384-d, (1966).

13. R. T. Quinn, R. W. Kraft and R. W. Hertzberg, "Structure and Elevated Temperature Mechanical Behavior of Unidirectionally Solidified Ni-Ni$_3$Nb Eutectic Alloy," Trans. ASM, v. 62, (1969), p. 38.

14. Ye M. Savitskiy, Ch. V. Kopetskiy and Ye P. Arskaya, "The Effect of Temperature on the Plastic Deformation and Mechanical Properties of Some Intermetallic Compounds," Russian Met. Mining, No. 6, (1964), p. 85.

15. R. T. Quinn, Structure and Elevated Temperature Mechanical Behavior of Unidirectionally Solidified Ni-Ni$_3$Nb Eutectic Alloy, Ph.D. Dissertation, Lehigh University, (1967).

16. I. J. Dueden and W. Hume-Rothery, "The Equilibrium Diagram of the System Niobium-Nickel," J. Less-Common Metals, v. 11, (1966), p. 381.

17. B. D. Cullity, Elements of X-ray Diffraction, Addison-Wesley, (1959).

18. R. W. Hertzberg, F. D. Lemkey and J. A. Ford, "Mechanical Behavior of Lamellar (Al-CuAl$_2$) and Whisker-type (Al-Al$_3$Ni) Unidirectionally Solidified Eutectics," Trans. AIME, v. 233, (1965), p. 1635.

19. M. Gell and G. R. Leverant, "The Fatigue of the Nickel-Base Superalloy MAR-M200, in Single-Crystal and Columnar-Grained Forms at Room Temperature," Trans. AIME, v. 242, (1963), p. 1869.

20. M. Gell and G. R. Leverant, "The Characteristics of Stage I Fatigue Fracture in a High Strength Nickel Alloy," Acta Met., v. 16, (1969), p. 553.
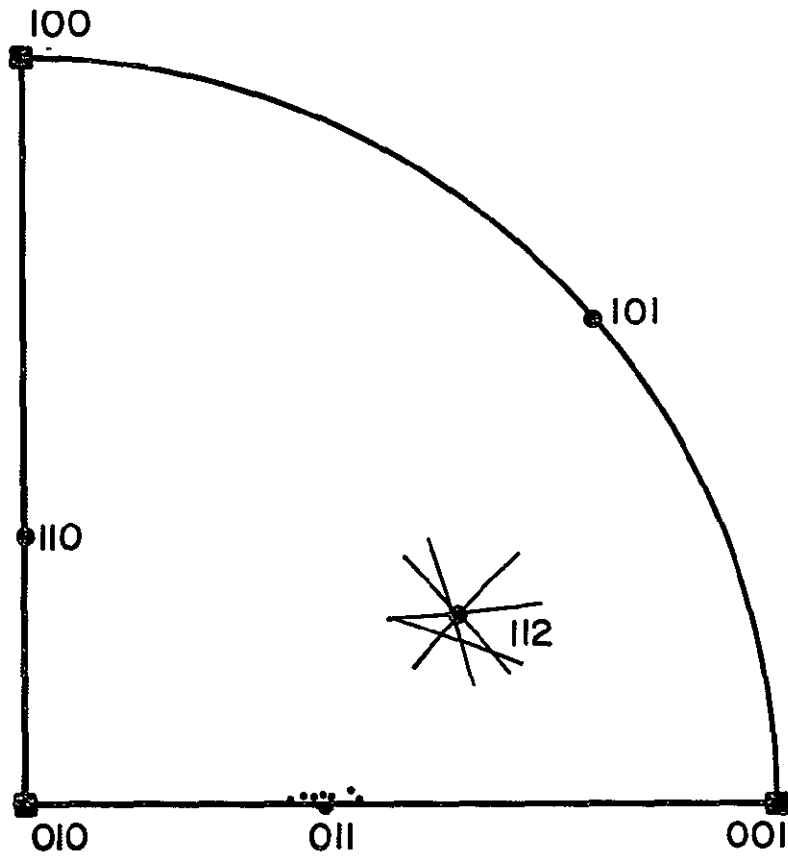
FIGURE 1: RESULTS OF TRACE ANALYSES INDICATING {112}
AND {011} TYPE Ni_3Nb DEFORMATION TWINS.
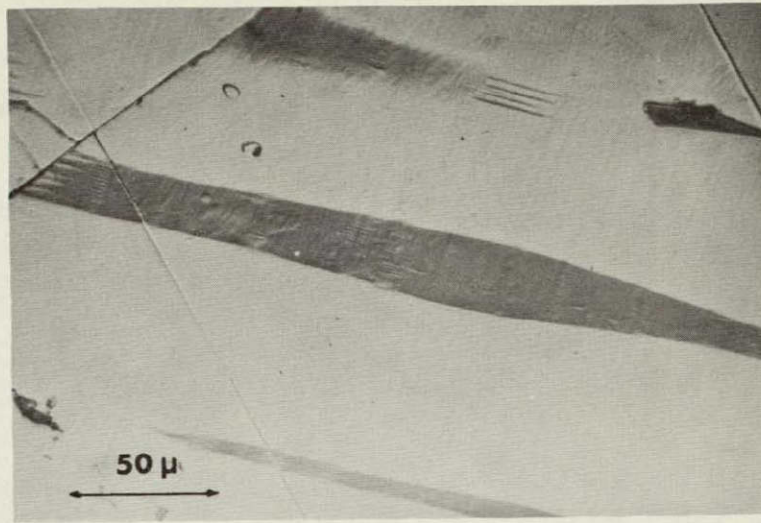
FIGURE 2: PHOTOMICROGRAPH SHOWING THE TYPICAL APPEARANCE
OF {011} TWINS IN Ni_3Nb (SURFACE RELIEF), 400X.

(a)   (b)
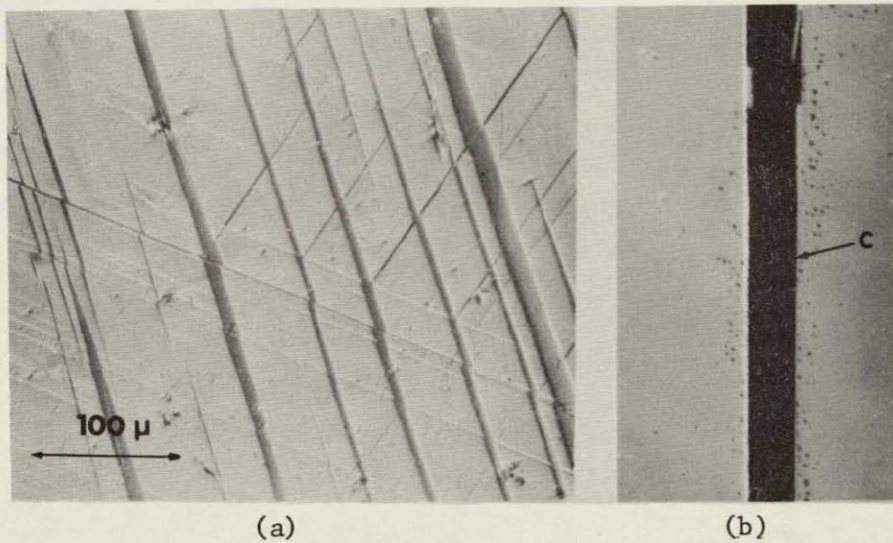
FIGURE 3: PHOTOMICROGRAPHS ILLUSTRATING THE TYPICAL APPEARANCE
OF {112} TWINNING IN Ni_3Nb. ("C" DENOTES A TWIN
BOUNDARY CRACK.) (a) SURFACE RELIEF, 200X;
(b) 400X.

43

FIGURE 4: PHOTOMICROGRAPH SHOWING THE DEFORMATION
SURFACE RELIEF DEVELOPED ON A PREPOLISHED
Ni$_3$Nb SPECIMEN RESULTING FROM COMPRESSIVE
LOADING, 50X.

44
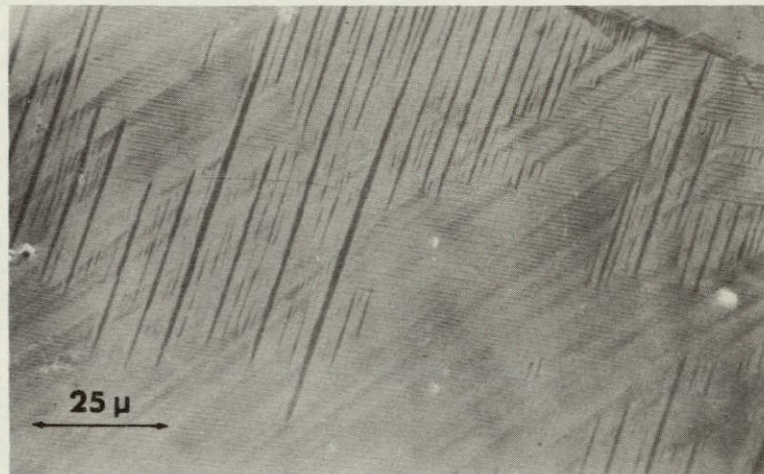
FIGURE 5: PHOTOMICROGRAPH SHOWING VERY FINE Ni$_3$Nb TWINS
(POLARIZED LIGHT, SURFACE RELIEF), 800X.
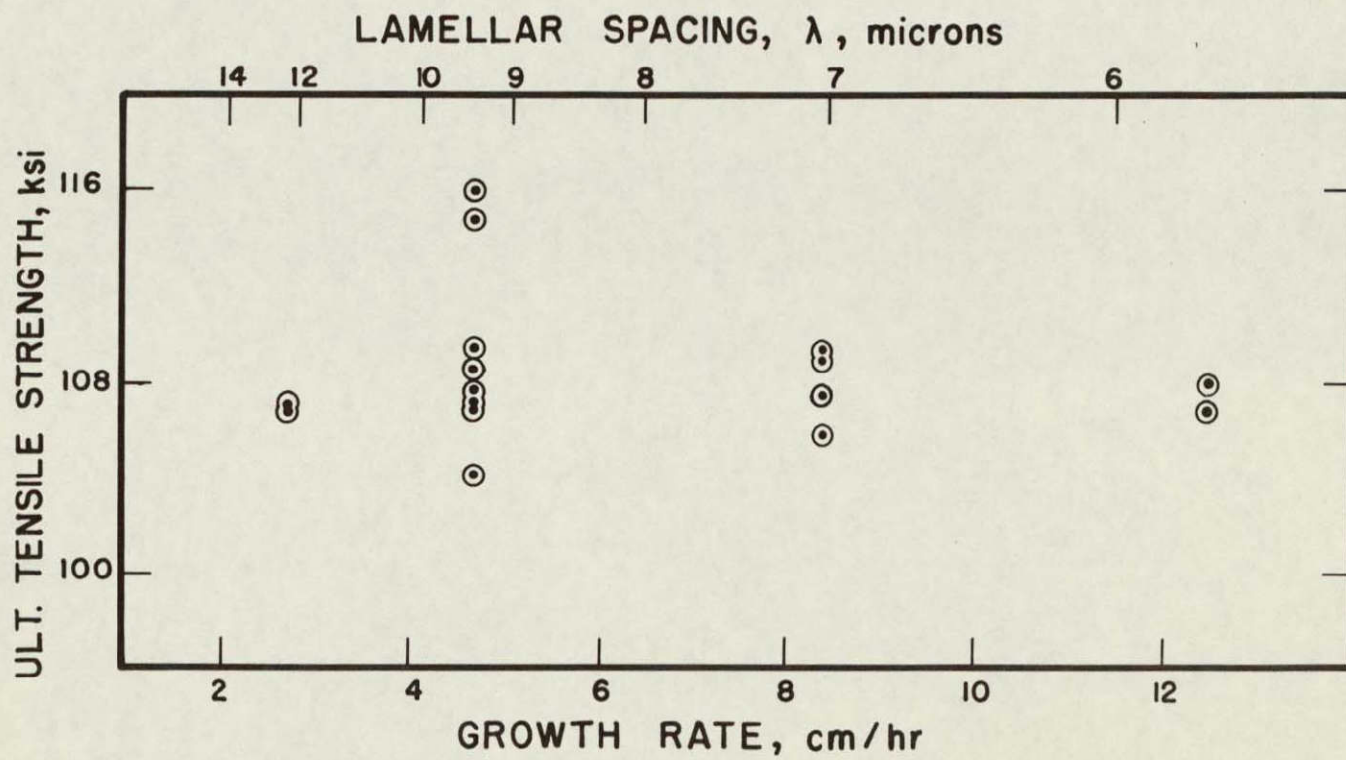
FIGURE 6: EFFECT OF GROWTH RATE ON ULTIMATE TENSILE STRENGTH FOR THE Ni-Ni$_3$Nb EUTECTIC COMPOSITE.
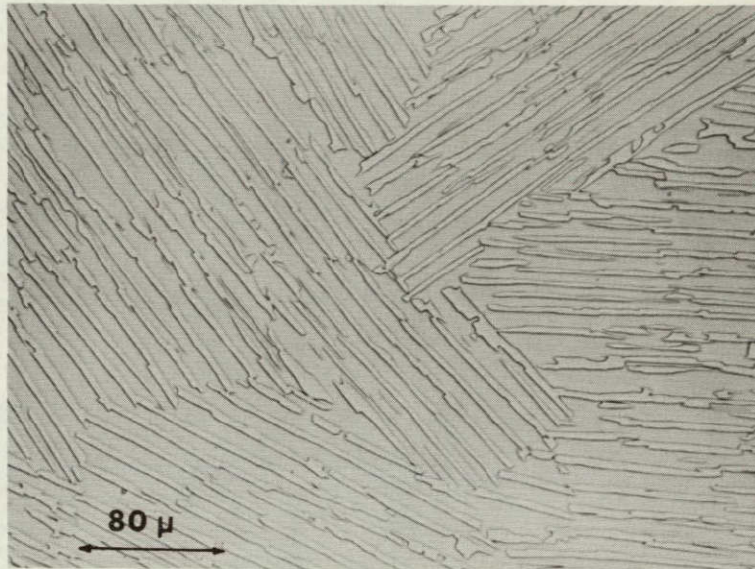
FIGURE 7: PHOTOMICROGRAPH REVEALING THE TRANSVERSE
STRUCTURE OF THE Ni-Ni$_3$Nb EUTECTIC COMPOSITE
(4.7cm/hr), 250X.

47
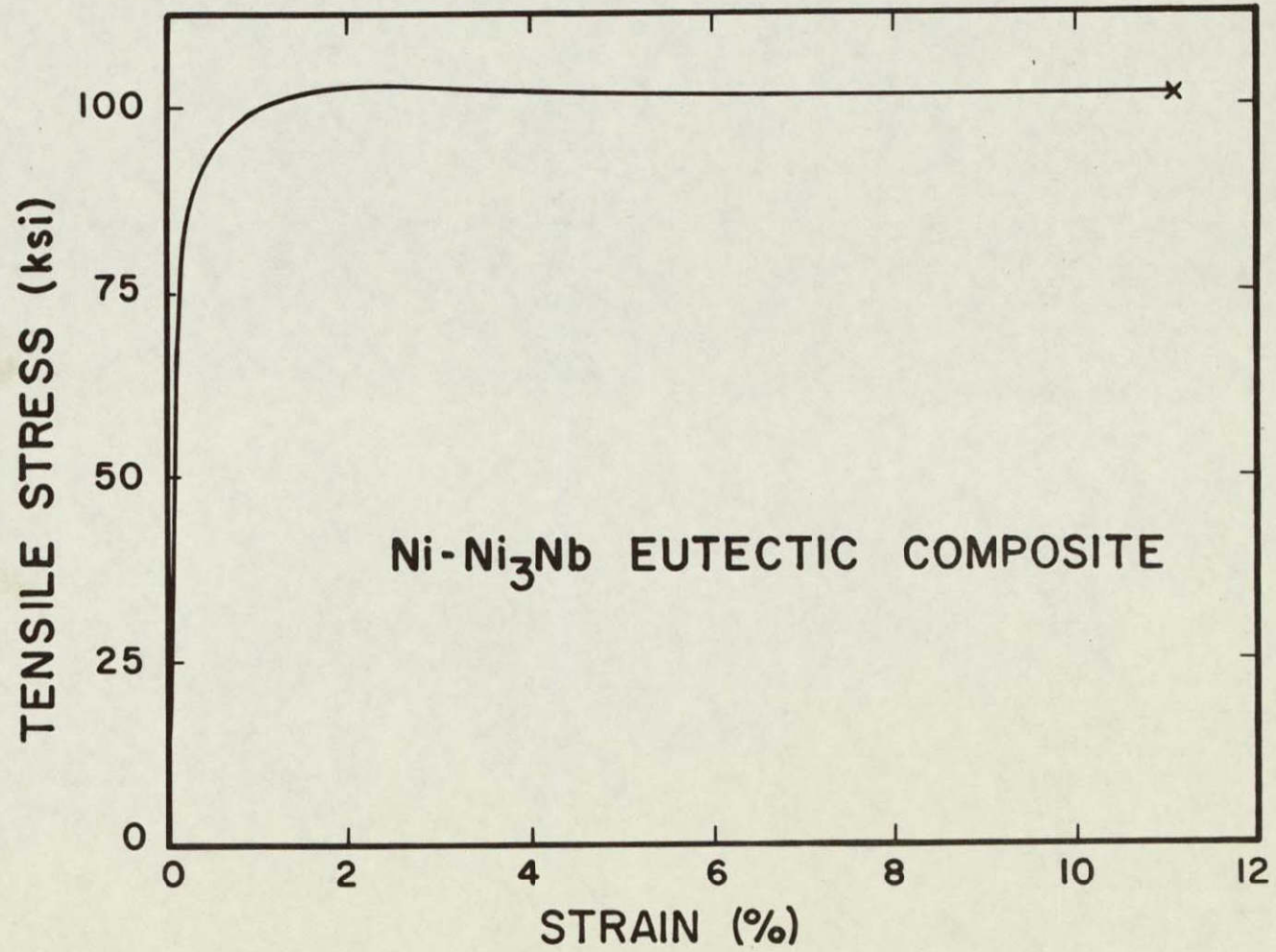
FIGURE 8: A TYPICAL TENSILE STRESS-STRAIN CURVE FOR THE Ni-Ni3Nb EUTECTIC COMPOSITE.
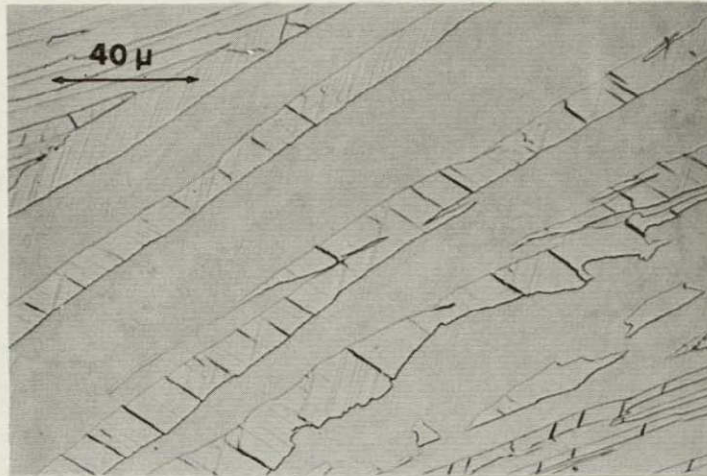
FIGURE 9: PHOTOMICROGRAPH SHOWING DEFORMATION TWINNING
AND TWIN BOUNDARY CRACKING DEVELOPED IN THE
Ni$_3$Nb PHASE OF THE EUTECTIC UNDER TENSILE
LOADING, (METALLOGRAPHIC TECHNIQUE B), 490X.

49
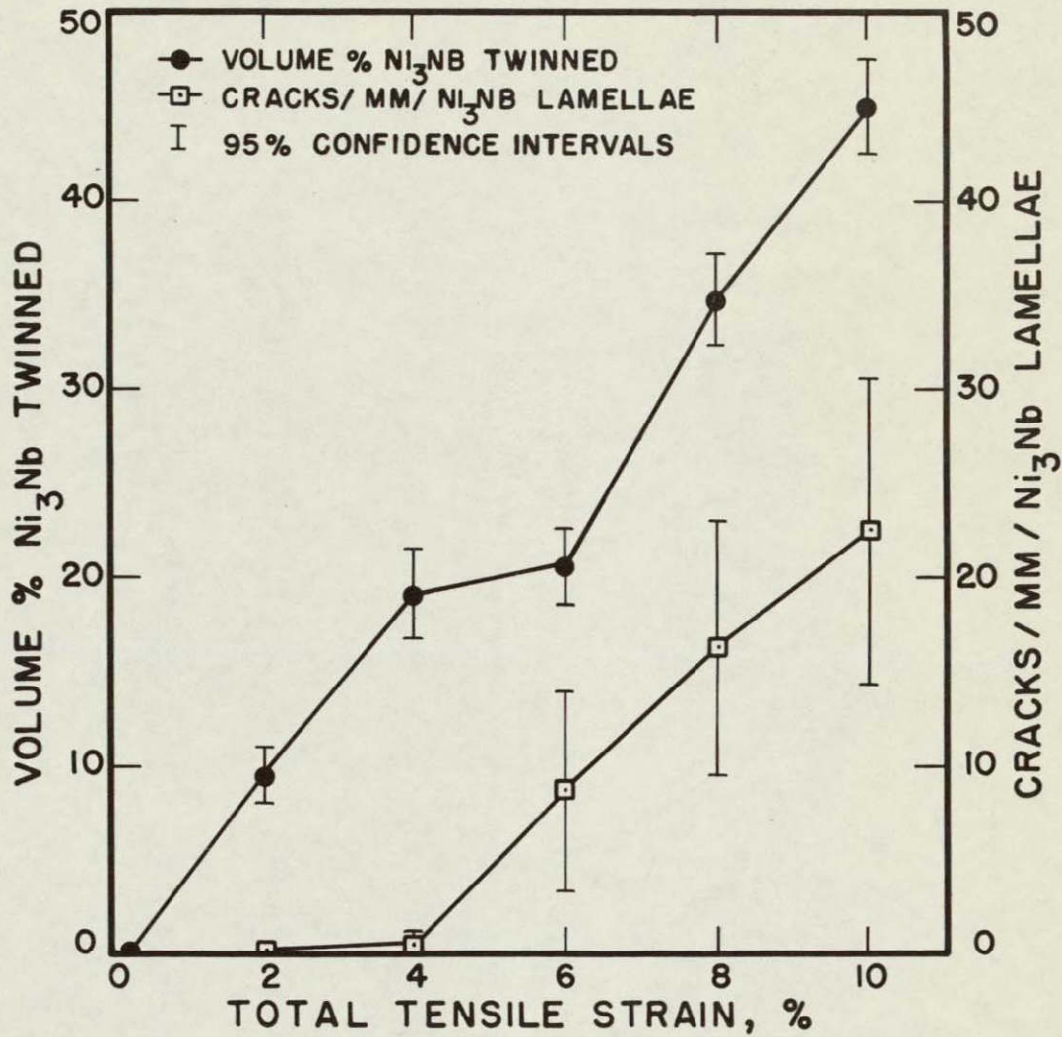
FIGURE 10: EXTENT OF Ni₃Nb TWINNING AND TWIN BOUNDARY CRACKING AS A FUNCTION OF COMPOSITE TENSILE STRAIN.

50
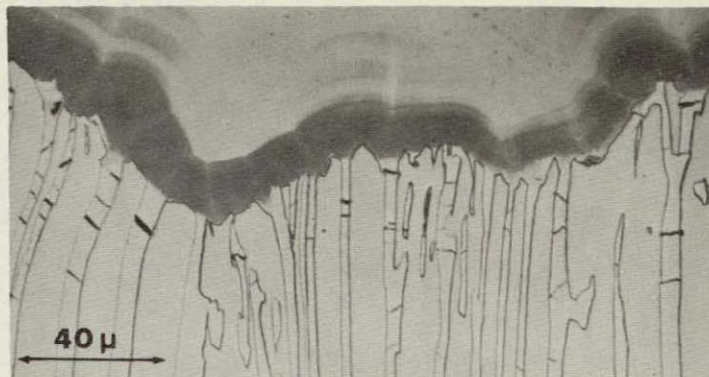
FIGURE 11: TYPICAL METALLOGRAPHIC PROFILE OF A
Ni-Ni₃Nb TENSILE FRACTURE, 490X.

FIGURE 12: ELECTRON FRACTOGRAPH REVEALING THE
TYPICAL TENSILE FRACTURE APPEARANCE
OF THE Ni-Ni₃Nb COMPOSITE, 3580X.

51
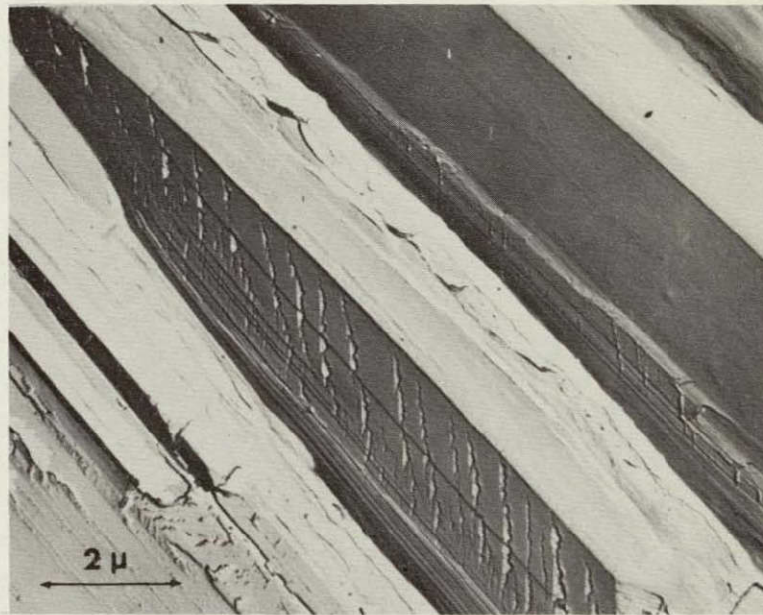
FIGURE 13: ELECTRON FRACTOGRAPH ILLUSTRATING THE TONGUES
AND STEPS FOUND ON Ni₃Nb FRACTURE SURFACES,
9,350X.
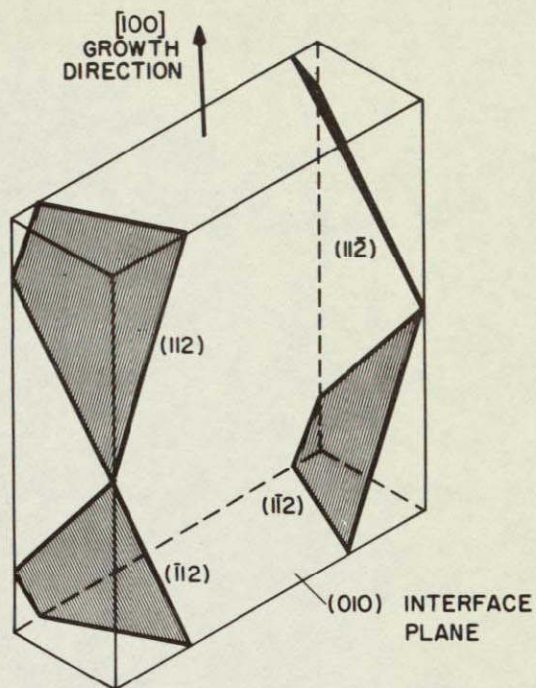
FIGURE 14: SCHEMATIC DRAWING OF THE ORIENTATIONS OF THE FOUR {112} TWIN VARIANTS IN A Ni_3Nb LAMELLAE.
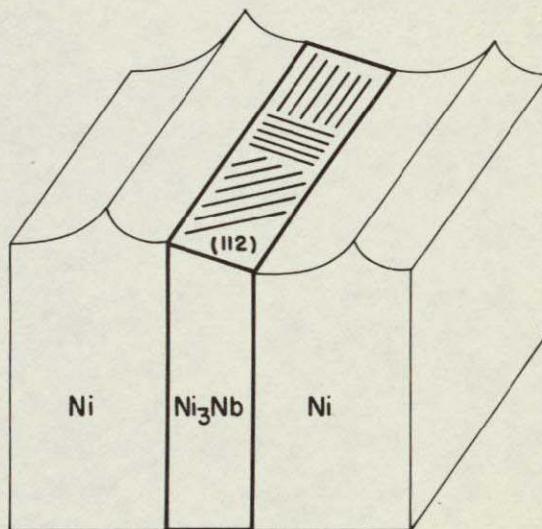
FIGURE 15: A SCHEMATIC ILLUSTRATION OF THE POSSIBLE INTERSECTIONS OF SECONDARY {112} TWINS WITH A {112} TWIN BOUNDARY FRACTURE SURFACE.

53
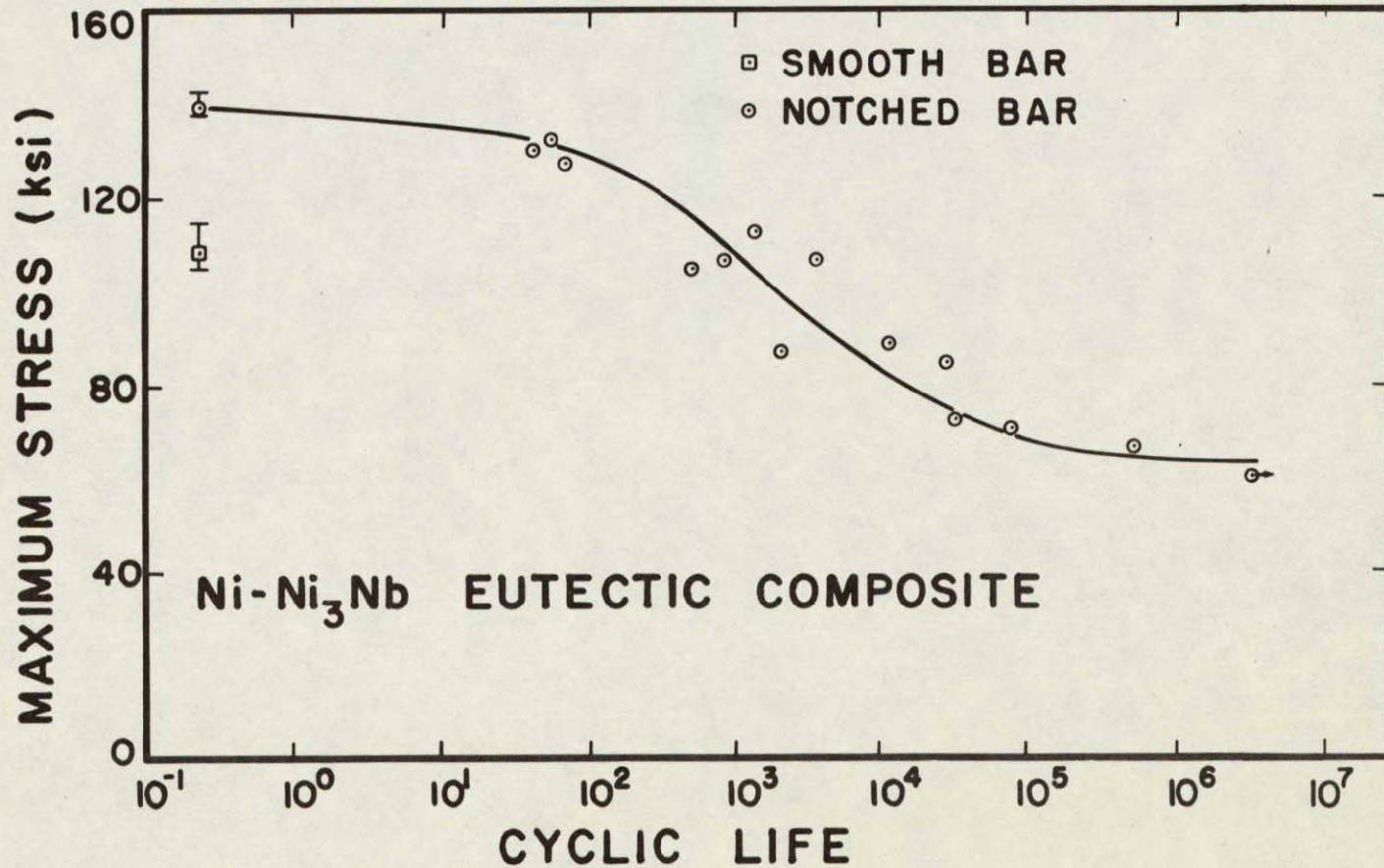
FIGURE 16: THE MAXIMUM NET SECTION STRESS VS. CYCLIC LIFE CURVE RESULTING FROM TENSION-TENSION FATIGUE TESTING OF THE Ni-Ni3Nb EUTECTIC COMPOSITE. ALL TESTING WAS CONDUCTED WITH A MINIMUM NET SECTION STRESS OF +2 ksi.
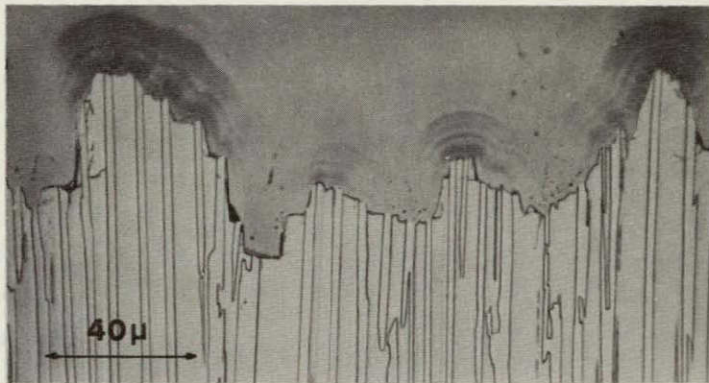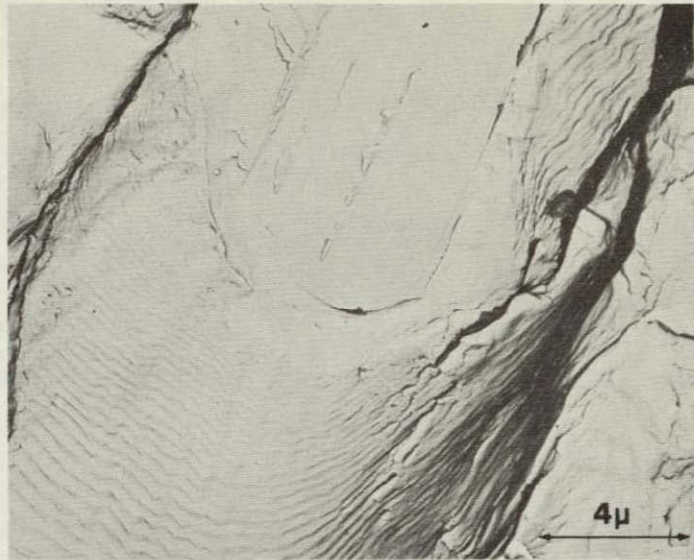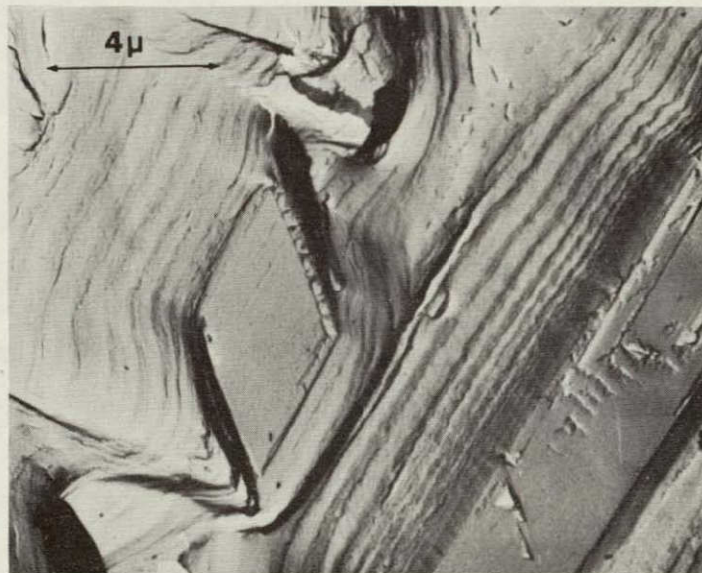
FIGURE 17: METALLOGRAPHIC PROFILE OF LOW STRESS-
HIGH CYCLE FATIGUE FRACTURE (562,800 CYCLES
TO FAILURE) SHOWING A LACK OF SECONDARY TWIN
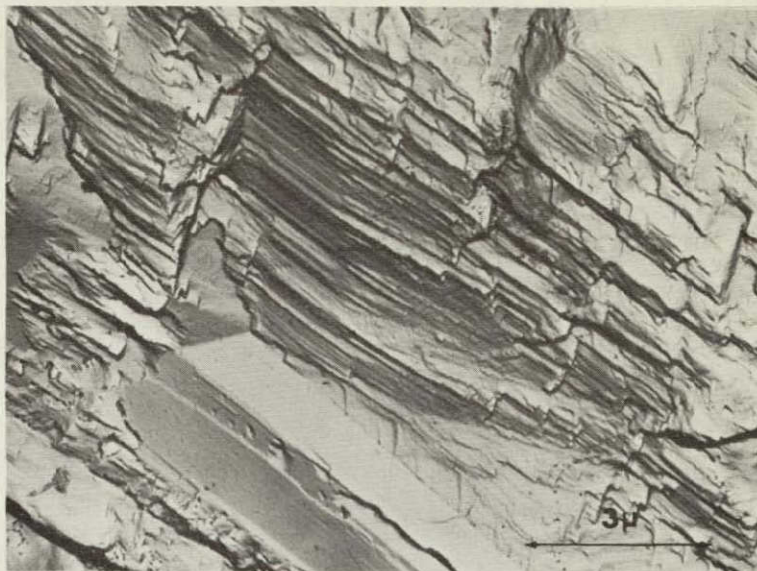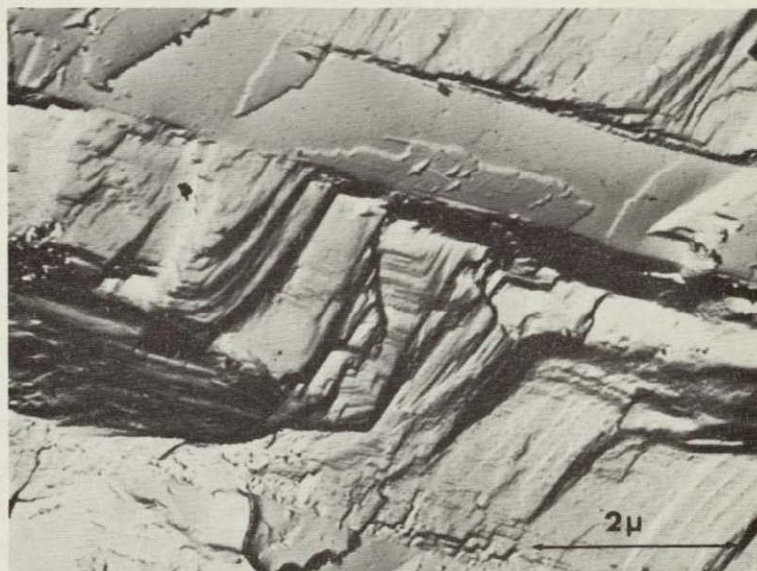BOUNDARY FISSURES, 490X.

(a)

(b)

FIGURE 18: ELECTRON FRACTOGRAPHS REVEALING STRIATIONS
PARALLEL TO THE Ni-Ni$_3$Nb INTERFACE UNDER
HIGH STRESS FATIGUE CONDITIONS:
(a) 5,050X; (b) 5,700X.

56

FIGURE 19: STRIATIONS FORMED UNDER INTERMEDIATE
LEVELS OF ALTERNATING STRESS WHICH
ASYMPTOTICALLY APPROACH THE Ni-Ni$_3$Nb
INTERFACE AS ILLUSTRATED IN AN ELECTRON
FRACTOGRAPH, 5,550X.

57

(a)

(b)

FIGURE 20: ELECTRON FRACTOGRAPHS REVEALING FACETED
Ni FRACTURE SURFACES UNDER HIGH CYCLE
FATIGUE CONDITIONS: (a) 8,400X;
(b) 13,900X.

VITA

William R. Hoover ███████████████████████████

████████████ to Dillon B. and Virginia ██████ Hoover. He received

his elementary and secondary education in the Edgewood School

System and was graduated from Edgewood High School in 1962. In

January, 1966, Mr. Hoover was married to the former Lois Elaine

Fletcher of Wilkinsburg, Pennsylvania.

In June, 1966, Mr. Hoover was graduated Cum Laude from

Lafayette College with a degree of Bachelor of Science in Metal-

lurgical Engineering. During his years at Lafayette, he was elected

to Tau Beta Pi, Phi Beta Kappa and Alpha Sigma Mu honorary fraterni-

ties, mentioned on the Dean's List and received the Luther F. Wit-

mer Prize for Metallurgy and the Carl J. Staska Prize in Engineering

and Chemistry.

Upon completion of his undergraduate studies, Mr. Hoover con-

tinued his education at Lehigh University as a research assistant

working under Dr. R. W. Hertzberg and Dr. R. W. Kraft on NASA

research grant number NGR-39-007-007. In February, 1968, Mr.

Hoover was awarded the degree of Master of Science in Metallurgy

and Materials Science. The title of his thesis was "The Low Cycle

Fatigue Behavior of the Unidirectionally Solidified $Al-Al_3Ni$

Eutectic Alloy." This work was published under the title of "The

Fatigue Characteristics of Unidirectionally Solidified $Al-Al_3Ni$

Eutectic Alloy" in the <u>ASM Transactions Quarterly</u>.

After completion of his master's work, Mr. Hoover continued his graduate studies at Lehigh University. He was appointed an Instructor in the Department of Metallurgy and Materials Science in September, 1968 and served in this position until June, 1970. Mr. Hoover presented a paper entitled "The Fatigue Behavior of the $Ni-Ni_3Nb$ Eutectic Composite" at the 1969 Fall meeting of the Metallurgical Society of the AIME.

Mr. Hoover will become a member of the technical staff of the Sandia Corporation at the Sandia Laboratories in Albuquerque, New Mexico upon termination of his doctoral studies.